19th Australasian Fluid Mechanics Conference
Melbourne, Australia
8-11 December 2014

Intermittency in the Outer Region of Turbulent Boundary Layers

K. A. Chauhan, R. Baidya, J. Philip, N. Hutchins and I. Marusic

Department of Mechanical Engineering, The University of Melbourne, Victoria 3010, Australia

Abstract

Characteristics of external intermittency in the outer region of turbulent boundary layers are presented based on single-point hotwire measurements. The distinction between the turbulent and non-turbulent state of the flow is marked by applying a threshold on instantaneous kinetic-energy, and this criteria is found to be adequate for this study. Mean intermittency profiles are in consistent agreement with previous observations. Further, conditionally averaged profiles of the streamwise velocity and its standard deviation show good agreement with scaling proposed by Chauhan *et al.* [3]. Probability density functions of the lengths of turbulent/non-turbulent zones show a range of intermediate scales over which power-law scaling is observed. The observed power-law scaling provides further evidence for a fractal geometry of the turbulent/non-turbulent interface (TNTI) over a wide range of Reynolds number and scale separation [8]. Finally, longer lengths (streamwise extent greater than $\delta/4$, where δ is the layer thickness) exhibit exponential probability distribution, indicating that a long turbulent/non-turbulent state occurs in the flow independent of the length of the alternate state preceding it.

Introduction

Corrsin & Kistler [6] first proposed the existence of a 'laminar super-layer' within which viscous forces transfer mean and fluctuating vorticity to the non-turbulent fluid. Thereafter substantial research in the 1970s and 80s focussed on the TNTI using hotwire measurements. Some notable studies in boundary layers that are relevant to our study are briefly mentioned here. Fiedler & Head [9] utilised smoke visualisation along with hotwire and Pitot tube measurements to conclude that the mean intermittency distribution is dependent on streamwise pressure gradient but not Reynolds number. The characteristics of the leading and trailing edges of the turbulent bulges in the outer part of the boundary layer were examined in Hedley & Keffer [10]. They found that sharp changes occur through the 'backs', while the 'fronts' exhibit a more diffusive behaviour. Chen & Blackwelder [5] confirmed the presence of a sharp interface by conditional averages of temperature profiles. Statistical properties of turbulent/non-turbulent zone lengths were examined by LaRue & Libby [14], who found an exponential distribution for large lengths, and by Tsuji *et al.* [18] who found a power-law behaviour of the distribution for the intermediate lengths. We shall revisit some of these characteristics of external intermittency and discuss their scaling using single hotwire measurements in a high Reynolds number facility. Particularly, results for mean intermittency, conditionally averaged profiles and probability density functions of turbulent/non-turbulent zone lengths will be presented.

Experimental Database

Single-point streamwise velocity measurements are acquired with a hot-wire in the high Reynolds number boundary layer wind tunnel (HRNBLWT) at the University of Melbourne. The present set of measurements are appended by measurements of Mathis *et al.* [15] and Kulandaivelu [13] in the same facility. Parameters relevant to this study are listed in table 1. For the current measurements, profiles were obtained at uniformly spaced wall-normal heights at each streamwise location; unlike the previous measurements where the wall-normal spacing is logarithmic. Uniform wall-normal spacing provides more locations in the outer region of the flow where statistics can be examined at any desired value of mean intermittency γ. Also it should be noted that for these measurements the acquisition time is considerably larger than that would be typically needed to obtain converged first- and second-order statistics. Longer acquisition times are particularly required to obtain converged results for probability density of long turbulent/non-turbulent zone lengths. The spatial resolution of a 2.5μm diameter hotwire varied from 11 to 31 viscous units. The details of the wind-tunnel and the experimental set-up can be found in references [15] and [13].

U_∞ ($\mathrm{m\,s^{-1}}$)	δ (m)	u_τ ($\mathrm{m\,s^{-1}}$)	$T = T_s \cdot U_\infty/\delta$	F_s (kHz)	Re_τ ($\delta u_\tau/\nu$)
10	0.38	0.33	7964	50	8079
15	0.37	0.48	24144	50	11558
20	0.36	0.64	16698	50	14771
25	0.35	0.78	21755	50	16999
30	0.34	0.92	26672	50	19672

Table 1. Experimental parameters for measurements in HRNBLWT. U_∞ is freestream velocity, δ is boundary layer thickness (based on a fit to composite profile of [4]), u_τ is skin-friction velocity, T_s is acquisition time, T is equivalent boundary layer turn-over time, F_s is sampling frequency and Re_τ is the friction Reynolds number or the Kármán number.

Detection of Turbulent/Non-turbulent Zones

Detection of intermittency from a velocity signal, i.e. identifying turbulent and non-turbulent regions in the flow, relies on establishing a kinematic criteria based on at least one component of velocity. The time derivative of the velocity, the derivative of the instantaneous shear stress or the magnitude of the velocity itself are the commonly used detector functions (see Hedley & Keffer [11] for a list of various functions used in past). In this study we use a criteria that is a measure of the instantaneous turbulent kinetic energy. Consider the streamwise velocity signal $\tilde{U}(t)$ in figure 1(a) that is non-turbulent for some time intervals and turbulent for the remaining time. In the outer part of the boundary layer, the convection velocity of the non-turbulent flow can be considered as U_∞ (indicated by the dashed line over $\tilde{U}$ in figure 1a). Over the non-turbulent regions, the fluctuations relative to U_∞, i.e. $\tilde{U} - U_\infty$ will be of the order of the freestream turbulence intensity, while in the turbulent regions of the signal $\tilde{U} - U_\infty$ fluctuations will be essentially much larger than the freestream intensity. Therefore, we consider a detector function $\tilde{Q}(t) = [1 - \tilde{U}(t)/U_\infty]^2$, as shown in figure 1(b), that is nearly zero (or of the order of freestream turbulence intensity) in the non-turbulent region and highly positive in the turbulent region. Based on the known freestream intensity in the tunnel, a threshold of 0.05 is adopted to represent $\tilde{Q}$ in a binary form $\tilde{I}(t)$ in figure 1(c). This choice of threshold is made to achieve a *Re*-independent collapse of intermittency profiles, an approach elaborated in [2]. In the turbulent part of the signal when $\tilde{Q} \geq 0.05$, $\tilde{I} = 1$ and when $\tilde{Q} < 0.05$, $\tilde{I} = 0$ in the non-turbulent part. An advantage of our approach is that a particular chosen threshold value is applicable to detect T/NT zones at

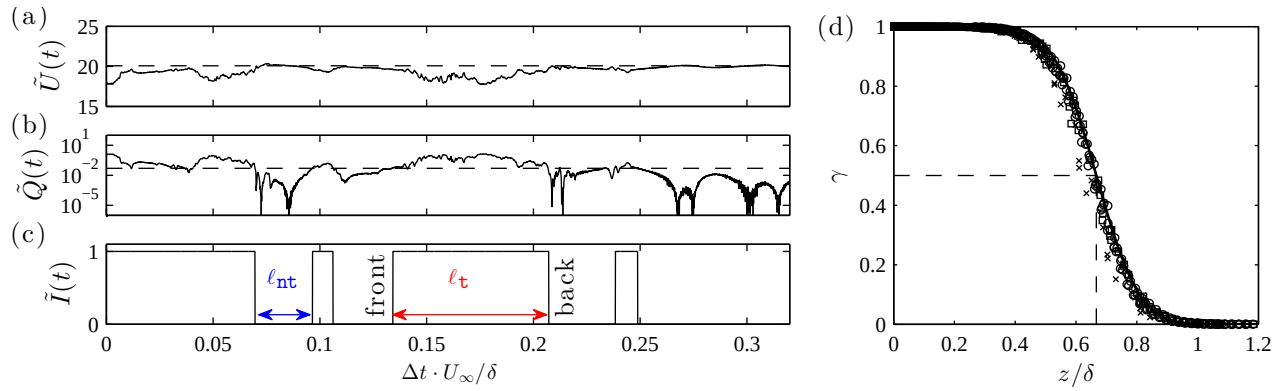

Figure 1. (a) Example instantaneous streamwise velocity measured by a hot-wire. Dashed line indicates the freestream velocity. (b) Corresponding detector function $\tilde{Q}(t)$. Dashed line is the cut-off for identifying turbulent/non-turbulent zones. (c) Binary intermittency signal. Value one corresponds to turbulent and zero to non-turbulent states. (d) Average intermittency function. $\gamma = 0.5$ occurs at $z/\delta \approx 2/3$ in zero-pressure-gradient turbulent boundary layers. '×', [15]; '□', [13]; '○', present. Solid line shows equation (2).

all wall-normal distances in the boundary layer. This approach is also applicable to PIV data where limited spatial resolution and/or noise in the data restricts use of derivative based methods for interface detection. The suitability of using a kinetic-energy criteria is evident in the results of Refs. [8, 2, 3]. The intermittency γ at a wall-normal position where the signal is acquired is then calculated as,

$$\gamma = \frac{1}{T_s}\int_0^{T_s} \tilde{I}(t)\,\mathrm{d}t, \tag{1}$$

where T_s is the total sampling time. It is well-known that the profile of $\gamma(z)$ in a zero-pressure gradient turbulent boundary layer is accurately described by the error function, [6, 9, 10, 5, and others].

$$\gamma(z) = \frac{1}{\sigma_i\sqrt{2\pi}}\int_z^{\infty} \exp\left[-\frac{(z-Z_i)^2}{2\sigma_i^2}\right]\mathrm{d}z \tag{2}$$

Here, Z_i is the mean interface location, i.e. a wall-normal position where $\gamma = 0.5$ and σ_i is the standard deviation of instantaneous interface position z_i relative to the mean position Z_i. Figure 1(d) plots 15 profiles of $\gamma(z)$ against the normalized wall-normal distance z/δ, spanning a Reynolds number Re_τ range of 2 740-22 900. It is observed that $Z_i/\delta \approx 2/3$ and $\sigma_i/\delta \approx 1/9$ at high Reynolds numbers [2]. The collapse of data in figure 1(d) and their agreement with error function (with $Z_i = 2\delta/3$ and $\sigma_i = \delta/9$) affirms our approach of detecting intermittency based on the $\tilde{Q}$ criteria and the chosen threshold.

Results

The turbulent/non-turbulent interface across which a detector probe leaves the non-turbulent flow and enters the turbulent flow is termed as 'fronts', while the T/NT interface where a probe leaves the turbulent region and enters the non-turbulent region is termed as 'backs'. In figure 1(c), the instantaneous intermittency signal $\tilde{I}$ changes from 0 to 1 at the fronts and from 1 to 0 at the backs. The properties of the superlayer at the TNTI can be examined by studying the measured quantities at the fronts and backs. From the available data we utilize conditional averaging as a tool to accomplish this.

Conditional Averages

Conditional averages of streamwise velocity $\langle\tilde{U}\rangle$ in the immediate vicinity of a front (in red) or a back (in blue) are plotted for measurements with $Re_\tau > 5000$ in figure 2(a). The conditional averages are for signals with mean intermittency $\gamma \approx 0.5$ which corresponds to a location where $z/\delta \approx 2/3$ (see figure 1d). The abscissa in figure 2 is equivalent streamwise distance from a front or a back calculated using Taylor's hypothesis and normalized with inner scaling ν/u_τ. We first identify each location of a front or back in the time signal and collect the velocity at those locations to calculate the average; this average value corresponds to the data-point at $\Delta t = 0$ in figure 2. Averages at a further lead/lag (non-zero Δt) relative to the fronts or backs are similarly obtained. One can clearly see that there is a steep change in streamwise velocity as one crosses the T/NT interface, as also previously observed by Chen & Blackwelder [5]. Deep in the turbulent region the velocity profile has a linear behaviour. The slope of profiles deviates from this linear behaviour and increases as one approaches the T/NT interface and again decreases to near-zero in the non-turbulent region. The change in slope occurs over a thin region at the interface indicative of the presence of a superlayer. If one extrapolates the linear trend of $\langle\tilde{U}\rangle$ from the turbulent and non-turbulent regions to $\Delta t = 0$, it is clear that a sudden jump in velocity has to occur across the interface. A jump in streamwise velocity across the TNTI has also been observed in jets [19, 7], wakes [1] and boundary layers [3], however these studies examine the conditional profiles in a direction perpendicular to the mean flow. Here, a steep change of velocity with time is detected at a fixed position in the outer flow. The similar behaviour of profiles in figure 2(a) with averages in the wall-normal direction suggests that it is likely that a steep change in velocity across the interface is independent of the orientation of the interface. Two-dimensional measurements, such as PIV, would assist in clarifying this, although one would require a large ensemble of vector fields to have converged results that are comparable to those from hot-wire measurements, especially for large lengths. It is noted that the magnitude of change in conditional velocities across the TNTI in figure 2 is in good agreement with the proposed scaling of the jump by Chauhan *et al.* [3], i.e. the deficit of the conditional streamwise velocity normalized by u_τ is $O(1)$.

The conditional profiles for standard deviation of the streamwise velocity relative to the conditional mean in figure 2(a) are plotted in figure 2(b). As expected the fluctuation levels are much higher in the turbulent region than the non-turbulent region across both fronts and backs. The steep rise in fluctuation intensity from the non-turbulent to turbulent region occurs in a region where the steep change in mean velocity also is found to occur. These profiles are similar to the fluctuation statistics averaged in the wall-normal direction [3]. Furthermore, we have normalized the standard deviation of conditional fluctuations with the local skin-friction velocity u_τ and find that there is no apparent Reynolds number trend observed. This implies that u_τ is an appropriate scaling velocity for the fluctuations, consistent with the conclusions made by Chauhan *et al.* [3].

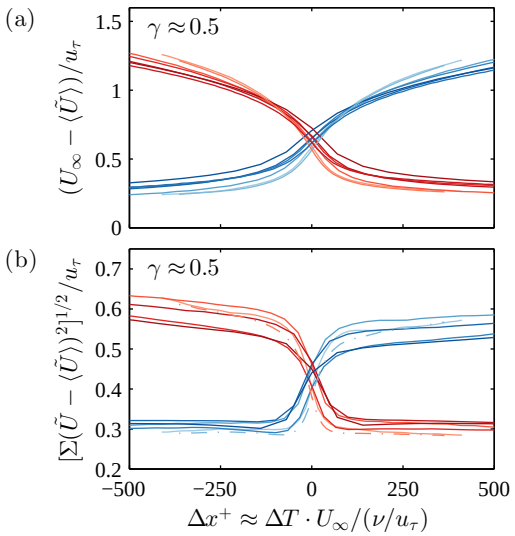

Figure 2. Conditionally averaged profiles across the turbulent/non-turbulent interface. A detected change from turbulent to non-turbulent state and vice-versa is at $\Delta x = 0$. Profiles in red, averaged at the fronts; profiles in blue, averaged at the backs. (a) conditionally averaged velocity relative to the freestream. (b) standard deviation of fluctuations relative to the conditional averages in (a). Shades of red and blue are darker with increasing *Re*.

Probability Distribution of Zone Lengths

In figure 1(c) the length of a turbulent and a non-turbulent segment of the signal is denoted by ℓ_{T} and ℓ_{NT}, respectively. Previous observations suggest that both ℓ_{NT} and ℓ_{T} are organized randomly in the signal and do not favour a particular organization of occurrence [12]. However, the statistical properties of ℓ_{NT} and ℓ_{T} are important to understand the organisation of large-scale structures associated with entrainment and whether the turbulent or non-turbulent events are associated with the large-scale motions underneath. Figure 3 plots the probability density of ℓ_{T} and ℓ_{NT} calculated from the $\tilde{U}$ signal at a wall-normal position where $\gamma = 0.5$ in a boundary layer. It is seen that both turbulent and non-turbulent zones occur at a wide range of scales and for $\gamma = 0.5$ have equivalent distribution; i.e. a characteristic measure (such as mean) of ℓ_{T} is equal to a similar characteristic measure of ℓ_{NT}. Intuitively, as one approaches the wall ($\gamma < 0.5$) the length of turbulent zones will become larger and the characteristic length of ℓ_{T} would be larger than that of ℓ_{NT} [10]. Similarly, further out in the boundary layer, the characteristic length of non-turbulent zones would be larger.

A distinctly noticeable feature in figure 3 is the remarkable collapse of profiles to exhibit a Reynolds number independent power-law behaviour of $\mathcal{P}$ shown by a solid black line [18]. One explanation for this behaviour is due to the fractal geometry of the instantaneous three-dimensional surface characterizing the turbulent/non-turbulent interface. Within the range of scales over which the power-law scaling is observed, the geometry of the TNTI can be considered as self-similar. The power-law scaling occurs with an overall exponent equal to $-4/3$ which is in very good agreement with previously observed values of the exponent (e.g. [17, 16, 8]). The fractal scaling ceases below an inner cut-off or when approaching the spatial resolution of the data. The inner cut-off is of the order of Taylor microscale, λ_T and is the scale where profiles deviate from the power-law if the inner scale ν/u_τ is used for normalizing ℓ_{T} and ℓ_{NT} in figure 3 (inner scaled distribution not shown here). The outer cut-off is approximately $\delta/4$, estimated from probability distributions plotted in figure 3 which utilizes the outer scale δ for ℓ_{T} and ℓ_{NT}. Between these limits the data shows power-law scaling over one order of magnitude of scale-separation. Beyond the outer cut-off TNTI does not have a self-similar behaviour and the overall geometry of the surface representing the TNTI is dictated by large-scale features that are $O(\delta)$.

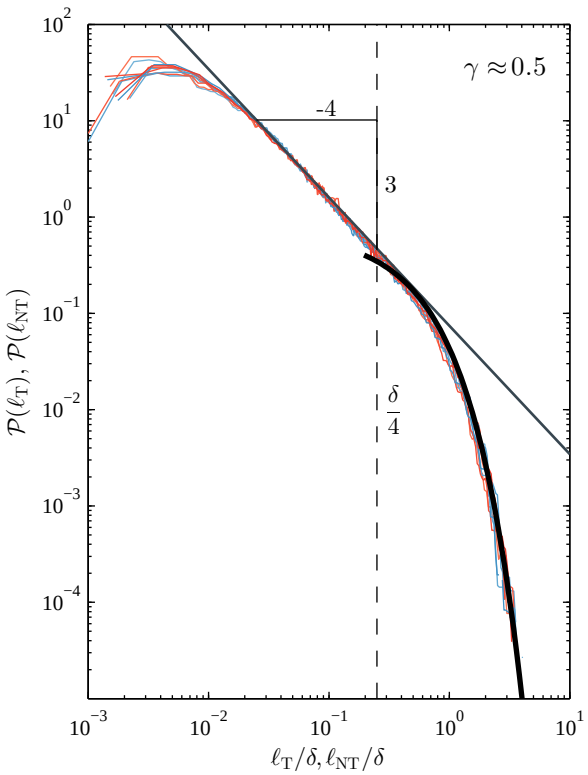

Figure 3. Probability distribution of turbulent (red) and non-turbulent (blue) zone lengths in outer scaling. Solid black line indicates an exponential distribution given by equation (3).

We also observe that in outer scaling the profiles for $\mathcal{P}$ collapse on to each other and have no *Re*-dependence even for zone lengths greater than $\delta/4$. The behaviour of $\mathcal{P}$ in this region is found to be exponential, as first suggested by Corrsin & Kistler [6]. Using hotwire measurements in the wake of a heated cylinder LaRue & Libby [14] also showed the exponential distribution of probability density functions of long zone lengths and our observations in the boundary layer consistently agree. The exponential distribution is plotted in figure 3 as the solid black line and given as

$$\mathcal{P}(l = x/4) = \lambda \cdot \exp(-\lambda x), \tag{3}$$

where λ is some parameter whose value is established later. Equation (3) is in very good agreement with the data. The probability that a zone length l is greater than some length $x_1/4$ is

$$\mathcal{P}[l \geq x_1/4] = \int_{x_1}^{\infty} \lambda \cdot \exp(-\lambda x)\,\mathrm{d}x = \exp(-\lambda x_1). \tag{4}$$

Now a hotwire signal consists of $N(= T_s \cdot F_s)$ discrete points. At a particular wall-normal height where the mean intermittency factor is γ, the probability that a single point in the signal is in a turbulent state is γ, while the probability that it is in a non-turbulent state is $1-\gamma$. The probability that a probe encounters at least K non-turbulent points before a turbulent state is detected is then

$$\mathcal{P}(n \geq K) = (1-\gamma)^K, \tag{5}$$

where n is number of points. Substituting $1-\gamma = \exp(-\lambda)$,

$$\mathcal{P}(n \geq K) = \exp(-\lambda K). \tag{6}$$

The above discrete probability is the same as expression (4) if $K = \lfloor x_1 \rfloor$; x_1 being a real number and K is the greatest integer

less than x_1. Therefore the parameter λ is equal to $-\ln(1-\gamma)$. It is also known that an exponential distribution has the property of being *memoryless*, i.e. the probability of a particular event occurring is independent of the prior events that have occurred. For the particular case of intermittent turbulent signal we can then say that the probability that a probe sees a turbulent/non-turbulent zone of certain length l is independent of the zone lengths preceding it. To prove this we consider that a turbulent/non-turbulent zone of length greater than l_1 has just passed the probe. The conditional probability of seeing a zone length $l \geq (l_1 + l_2)$ of alternate state (l_2 is some positive increment) is then $\mathcal{P}[l \geq (l_1+l_2) \mid l \geq l_1]$. (Note that $\mathcal{P}$ in equation 3 is the same for ℓ_{NT} and ℓ_{T} for $\gamma = 0.5$).

$$\mathcal{P}[l \geq (l_1+l_2) \mid l \geq l_1] = \frac{\mathcal{P}[l \geq (l_1+l_2) \cap l \geq l_1]}{\mathcal{P}[l \geq l_1]} \quad (7)$$

The numerator represents the combined probability of seeing a zone length greater than $l_1 + l_2$ and l_2, which is essentially the probability of seeing a zone length greater than $l_1 + l_2$.

$$\therefore \mathcal{P}[l \geq (l_1+l_2) \mid l \geq l_1] = \frac{\mathcal{P}[l \geq (l_1+l_2)]}{\mathcal{P}[l \geq l_1]}$$
$$= \frac{\exp\big(-4\lambda(l_1+l_2)\big)}{\exp(-4\lambda l_1)}$$
$$\therefore \mathcal{P}[l \geq (l_1+l_2) \mid l \geq l_1] = \exp(-4\lambda l_2) = \mathcal{P}[l \geq l_2]$$

Since the probability on the r.h.s. is independent of l_1, any arbitrary choice of l_1 can be made for the conditional probability on the l.h.s. as a zone length preceding $l_1 + l_2$. Thus $\mathcal{P}[l = l_2]$ is independent of l_1.

Finally, substituting $l = \ell/\delta$ and $x = 1$ in equation (4) gives $\mathcal{P}[\ell \geq \delta/4] = 0.5$. This implies that when $\gamma = 0.5$, 50% of the total signal consists of turbulent/non-turbulent zones that are greater than $\delta/4$ in length.

Conclusions

Intermittency characteristics are examined over a wide range of Reynolds number with *Re* exceeding any of the previous such studies. We find that the conditional statistics exhibit *Re*-independent scaling when inner normalization by u_τ and ν/u_τ is used as velocity and length scales, respectively. The probability density function for turbulent/non-turbulent zone lengths show fractal scaling at intermediate scales. The range of scales over which fractal behaviour is observed increase with increasing Reynolds number. For large zone lengths (exceeding $\delta/4$) existence of an exponential distribution is established clearly. The exponential distribution is indicative of random organisation of large-scale bulges/valleys in the outer part.

Acknowledgements

The authors acknowledge the financial support of the Australian Research Council.

References

[1] Bisset, D. K., Hunt, J. C. R. and Rogers, M. M., The turbulent/non-turbulent interface bounding a far wake, *J. Fluid Mech.*, **451**, 2002, 383–410.

[2] Chauhan, K., Philip, J., de Silva, C., Hutchins, N. and Marusic, I., The turbulent/non-turbulent interface and entrainment in a boundary layer, *J. Fluid Mech.*, **742**, 2014, 119–151.

[3] Chauhan, K., Philip, J. and Marusic, I., Scaling of the turbulent/non-turbulent interface in boundary layers, *J. Fluid Mech.*, **751**, 2014, 298–328.

[4] Chauhan, K. A., Monkewitz, P. A. and Nagib, H. M., Criteria for assessing experiments in zero pressure gradient boundary layers, *Fluid Dyn. Res.*, **41**.

[5] Chen, C. P. and Blackwelder, R. F., Large-scale motion in a turbulent boundary layer: a study using temperature contamination, *J. Fluid Mech.*, **89**, 1978, 1–31.

[6] Corrsin, S. and Kistler, A. L., Free-stream boundaries of turbulent flows, Tech. Rep. TN-1244, NACA, Washington, DC, 1955.

[7] da Silva, C. B. and Taveira, R. R., The turbulent/non-turbulent interface and viscous superlayer in turbulent planar jets, in *proceedings of 14th European Turbulence Conference*, 1-4 September, Lyon, France, 2013.

[8] de Silva, C. M., Philip, J., Chauhan, K., Meneveau, C. and Marusic, I., Multiscale geometry and scaling of the turbulent-nonturbulent interface in high Reynolds number boundary layers, *Phys. Rev. Lett.*, **111**, 2013, 044501.

[9] Fiedler, H. and Head, M. R., Intermittency measurements in the turbulent boundary layer, *J. Fluid Mech.*, **25**, 1966, 719–735.

[10] Hedley, T. B. and Keffer, J. F., Some turbulent/non-turbulent properties of the outer intermittent region of a boundary layer, *J. Fluid Mech.*, **64**, 1974, 645–678.

[11] Hedley, T. B. and Keffer, J. F., Turbulent/non-turbulent decisions in an intermittent flow, *J. Fluid Mech.*, **64**, 1974, 625–644.

[12] Kovasznay, L. S. G., Kibens, V. and Blackwelder, R. F., Large-scale motion in the intermittent region of a turbulent boundary layer, *J. Fluid Mech.*, **41**, 1970, 283–325.

[13] Kulandaivelu, V., *Evolution of zero pressure gradient turbulent boundary layers from different initial conditions*, Ph.D. thesis, The University of Melbourne, Melbourne, Australia, 2012.

[14] LaRue, J. C. and Libby, P. A., Statistical properties of the interface in the turbulent wake of a heated cylinder, *Phys. Fluids*, **19**, 1976, 1864–1875.

[15] Mathis, R., Hutchins, N. and Marusic, I., Large-scale amplitude modulation of the small-scale structures of turbulent boundary layers, *J. Fluid Mech.*, **628**, 2009, 311–337.

[16] Meneveau, C. and Sreenivasan, K. R., Interface dimension in intermittent turbulence, *Phys. Rev. A*, **41**, 1990, 2246.

[17] Sreenivasan, K. R., Ramshankar, R. and Meneveau, C., Mixing, entrainment and fractal dimensions of surfaces in turbulent flows, *Phil. Trans. Royal Soc. Lond.* A *Math. Phys. Sci.*, **421**, 1989, 79–108.

[18] Tsuji, Y., Honda, K., Nakamura, I. and Sato, S., Is intermittent motion of outer flow in the turbulent boundary layer deterministic chaos?, *Phys. Fluids A*, **3**, 1991, 1941.

[19] Westerweel, J., Fukushima, C., Pedersen, J. M. and Hunt, J. C. R., Momentum and scalar transport at the turbulent/non-turbulent interface of a jet, *J. Fluid Mech.*, **631**, 2009, 199–230.